MONITORING DEGRADATION OF WETLAND AREAS USING SATELLITE IMAGERY AND GEOGRAPHIC INFORMATION SYSTEM TECHNIQUES

A. H. Ali [1] H.S. Jaber [2]
Researcher Assist. Prof
[1]Engineering Department, Baghdad Governorate, Iraq,
[2]Department of Surveying Engineering, College of Engineering, University of Baghdad, Iraq,
alaahanoonali@gmail.com husseinsabah00@gmail.com

ABSTRACT

In order to conserve the ecosystems and biodiversity of wetland areas, it is necessary to monitor the degradation of these areas. Currently, Al Razzazah lake and its surrounding areas have degradation significantly due to its low water level, which has negatively affected its biodiversity. Hence, this research aims to propose a method to model the monitoring of spatio-temporal changes in that lake and its surrounding areas with an area estimated at 4660 km² between (1998 – 2018) using Remote Sensing and Geographic Information System (GIS) techniques. After conducting the supervised classification by the method of Support Vector Machine (SVM) for all satellite images, we extracted thematic maps, which contain five classes. The results showed the overall accuracy was 90.11%, 91.60% and 90.57% while the Kappa coefficient were 0.8764, 0.8950 and 0.8821 for 1998, 2008 and 2018 respectively. Results showed that the lake area decreased by 86.21% in the study area in 2018.

Keywords: wetland degradation; GIS; supervised classification; (SVM); thematic maps.
Part of M.Sc. thesis of the 1st author.

مراقبة تدهور مناطق الأراضي الرطبة بأستخدام تقنيات صور الأقمار الصناعية ونظم المعلومات الجغرافية

علاء حنون علي [1] حسين صباح جابر [2]
باحث استاذ مساعد
قسم الهندسة، محافظة بغداد، العراق [1]
قسم هندسة المساحة ، كلية الهندسة ، جامعة بغداد ، العراق[2]

المستخلص:

من أجل الحفاظ على النظم الإيكولوجية والتنوع البيولوجي في المناطق الرطبة، فمن الضروري رصد تدهور تلك المناطق. حاليا، بحيرة الرزازة والمناطق المحيطة بها تدهورت بشكل كبير بسبب أنخفاض منسوب المياه فيها، والتي أثرت سلبا على تنوعها البيولوجي. علاوة على ذلك، يهدف هذا البحث إلى اقتراح طريقة لنمذجة رصد التغيرات المكانية والزمانية في تلك البحيرة والمناطق المحيطة بها بمساحة تقدر ب 4660 كيلومتر مربع ما بين (1998–2018) باستخدام تقنيات الاستشعار عن بعد ونظم المعلومات الجغرافية (GIS). بعد إجراء التصنيف الموجه عليها وبطريقة خوارزمية (SVM) لجميع صور الأقمار الصناعية، تم استخراج الخرائط المواضعية، التي تحتوي على خمسة أصناف. أظهرت النتائج أن الدقة الإجمالية 90.11٪، 91.60٪ و 90.57٪ في حين أن معامل كابا 0.8764، 0.8950 و 0.8821 لعام 1998، 2008 و 2018 على التوالي. وأظهرت النتائج أن مساحة البحيرة انخفضت بنسبة 86.21٪ في منطقة الدراسة في عام 2018.

الكلمات المفتاحية : تدهورمناطق الاراضي الرطبة، نظم المعلومات الجغرافية، التصنيف الموجه، خوارزمية SVM ، الخرائط الموضوعية.

***جزء من رسالة ماجستير للباحث الأول.**

***Received:14/6/2019, Accepted:16/9/2019**

INTRODUCTION

Wetland, including lakes, rivers, swamps, rice fields, and marshes, is one of the most fertile ecosystems of biological production, providing food for fish, birds and animals as well as contribute to the provision of many services that increase human well-being and reduce poverty, particularly those living near these wetlands and are affected by the degradation of those areas (23) There are several reasons that led to the degradation of wetlands, which caused the reduction of its areas or areas of their existence, including natural and other man-made causes (14). Previous studies have shown that the area of wetlands has decreased significantly in the past 50 years due to the reclamation of wetlands, population pressure, water diversion, dam Construction, pollution, over-resources, biological invasion, desertification, climate change and Global warming as well as misguided policies (6,16). As referred by Tian etal. (24) it's necessary to strive to preserve those environments for the sustainability of life. On his part, (9), confirmed that studying deterioration and/or drought in water resources contributes greatly to exploring and analyzing the universal change of these wetlands in any part of the world. A study conducted by the United Nations (UN) in Iraq at 2013 has shown that many rivers and lakes in some countries have been heavily affected by dams and irrigation projects built in the headwaters of adjacent countries such as Turkey, Iran and Syria, particularly in Iraq (13),these study also noted, the continuous decline in water resources in Iraq is one of the major problems affecting the Iraqi ecosystem. Indeed, we have seen a decline in the last 10 years of water resources within our country, especially in the Tigris and Euphrates rivers, and its impact on the water reserves in the lakes, especially "Al Razzazah lake, as well as, the marshlands. Al Razzazah lake is a second largest lake in Iraq in terms of water storage, with a surface area of 1810 km² and a depth of about 30 m and a reservoir capacity of 26 billion m³ and its one of the main sources of fish wealth, a main source of irrigation for agricultural areas, and a "tourist attraction"(11). More recently, this lake is in a critical situation because of the reduce of water coming from Euphrates river through Habbaniyah lake because of the apprehensive fall of the water level in the Euphrates river due to the external water policies of the sources of rivers and non-compliance with the water shares of riparian countries (1,27). Meanwhile, climate changes, higher temperatures and higher levels of evaporation have resulted in a decrease in the water level and surface area and an increase in salinity (9). Furthermore, an area of 4,660 km² including Al Razzazah lake and its surrounding areas (case study) was selected to study and estimate the magnitude of those degradations.

MATERIALS AND METHODS

Study area and data used

The study area involves al Razzazah lake and its adjacent areas and covers an area of 4,660 km², the smallest part of which is located in the north-west side of Karbala province, while the largest part is located in al Anbar governorate and limited by longitudes 43 ° 19 '34″E to 43 ° 55' 31″E and latitudes 32 ° 23'18″ N to 33 ° 8'41″N. As shown in Figure 1.

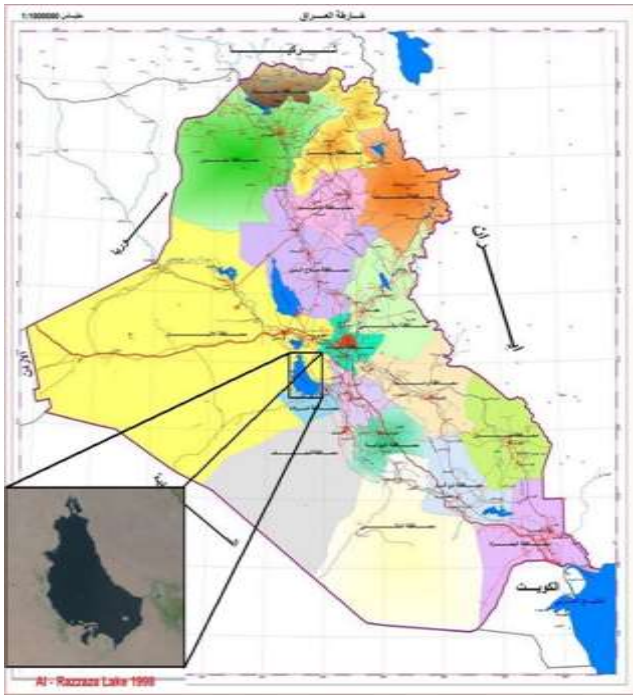

Figure 1 Study area map

The region has a dry climate in hot summers and its cold and dry in winter, resulting in a clearly reduced annual rainfall rate in the past three decades and an increase in average maximum and minimum temperatures, as shown in table 1, fulfilling in a significant increase in annual evaporation rate since 1970 (9).

Table 1. Climate data of the study area for years 1998, 2008 & 2018

Climate data	Year	Annual rate
Rainfall	1998	0.14 mm
Rainfall	2008	0.27 mm
Rainfall	2108	0.10 mm
Max temperature	1998	31.09 C°
Max temperature	2008	30.50 C°
Max temperature	2018	31.22 C°
Min temperature	1998	17.40 C°
Min temperature	2008	16.87 C°
Min temperature	2018	16.62 C°

The geology of study area contains of several sorts of soils as a result of a different geologic environment and fluvial processes. Includes gypsiferous gravel, sand dunes, tertiary sediments and rock units and the barren land, which is dry salt flats, Razzazah beaches, additionally, the water body includes shallow and deep water (19). Three satellite images were utilized to conduct this study for the period (1998 - 2018), as showing in Figures 2, 3&4. Two images obtained from the Landsat 5 TM in 9 August 1998 and 4 August 2008, and the third image downloaded from the Landsat 8 OLI in 16 August 2018, were gathered from the path 169 and row 37. As well as Quickbird satellite image for supporting the geometric correction process and increased visual ability in the interpretation of visual phenomena. It is worth mentioning, it can be obtained freely after registering at the USGS official website at https://earthexplorer.usgs.gov/

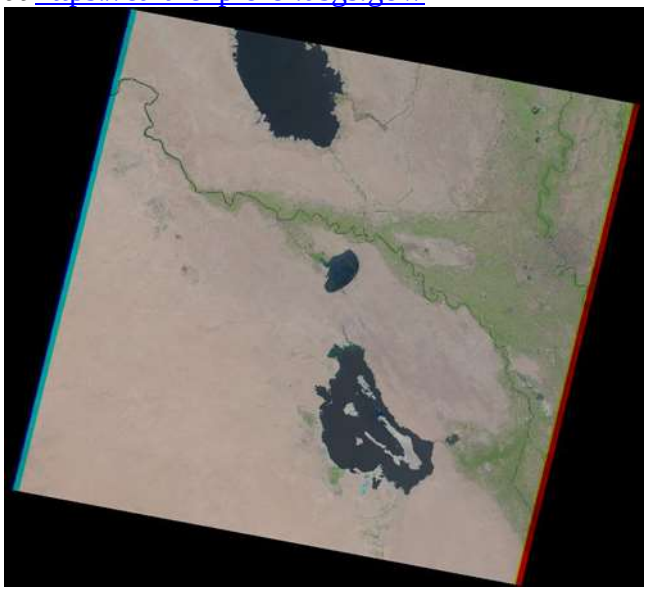

Figure 2. Landsat 5 TM image 1998 of the study area.

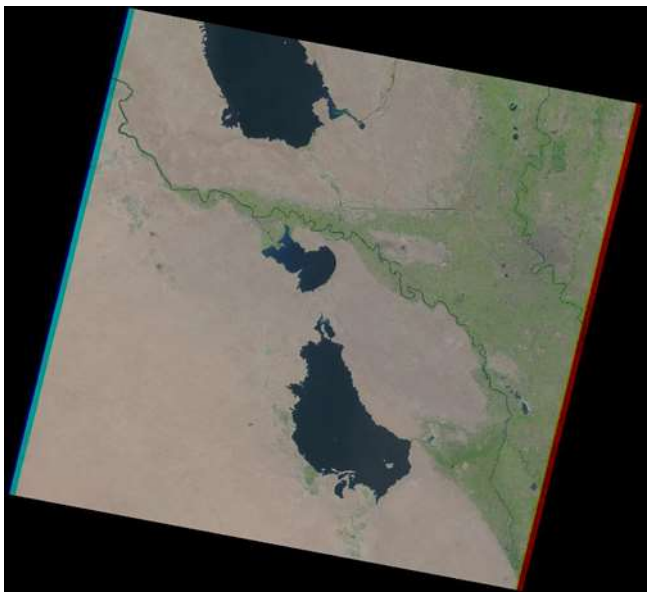

Figure 3. Landsat 5 TM image 2008 of the study area

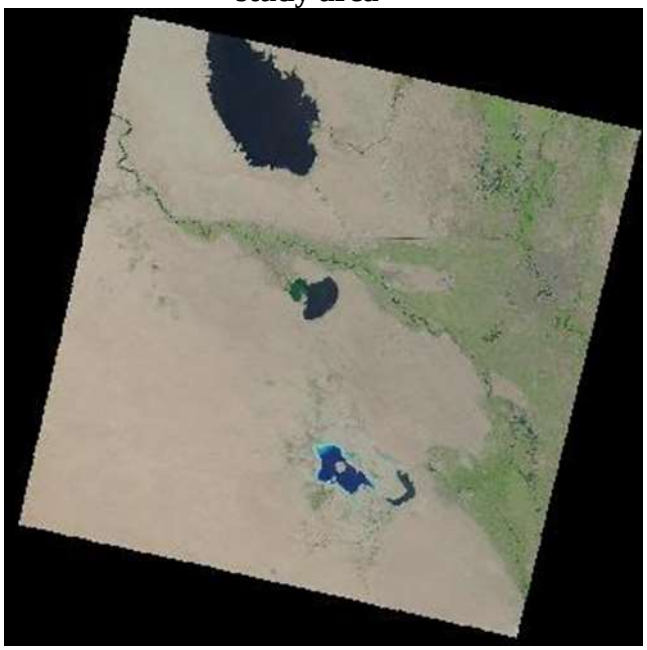

Figure 4. Landsat 8 OLI image 2018 of the study area

Methodology

The methodology followed in this study consists of several steps. The first step is very important of which are pre-processing raw data, including radiometric, geometric correction, as well as the co-registration process. The second step includes layer stacking and sub-setting, moreover, data are ready to be classified in the third step. After determining the elected classification categories and studying the case study well, the supervised classification of these corrected images was carried out by Support Vector Machine (SVM) algorithm using Environment for Visualizing Images (ENVI) 5.3v software.

The most prominent steps in the methodology can be summarized in the flowchart shown in Figure 5. After obtaining the thematic maps of all the images classified by Arc GIS 10.2v software in the fourth step, accuracy assessment was confirmed and compared to the global parameters as a fifth step, followed by the change detection process and statistical analysis as a final step in order to obtain the objectives and results of this research.

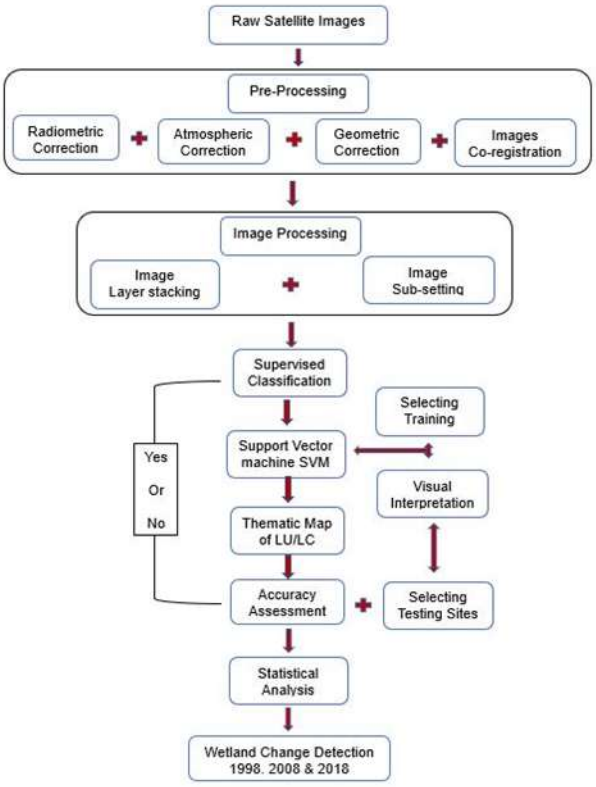

Figure 5. Flowchart of the all steps adopted in methodology of the research

It can be explained above steps as following:

Image pre-processing

These processes aim to correct distorted remote sensing data in order to obtain a more truthful representation of the real reality and to improve images for later use (12). As reported by (22), that several significant reasons lead to the calibration of satellite images, since raw sensor digital numbers (DNs) are just numbers without physical units and that each sensor has its own acquisitions and entitlements applied to registered signals to configure band names. Preprocessing is imperative, and includes a sequential operation such as radiometric, atmospheric and geometric corrections by achieving these operations, it is possible to correct image distortion and improve image quality and thus rise the feasibility of interpretation (22). We know that the solar radiation falling on the earth, part of it that is reflected and received by satellites in the layers of the atmosphere due to the presence of some particles (water vapor and dust, as well as some gases) and the other is penetrate the atmosphere to reach the surface of the globe to reflect a section of it once again the first type is called Path radiance (Lp) and the other type is outgoing radiance. As a result, satellite sensors record both types of light emission (12).

Measure Radiance Ltot = Path Radiance+ Outgoing Radiance

$L\ tot = (PET) / 2\pi + Lp$ ……... 1

Where:

Ltot = total spectral radiance measured by sensor

P = reflectance of object

E = irradiance on object

T = transmission of atmosphere

L = Outgoing Radiance

Lp = path radiance

From eq. 1

Outgoing Radiance = Measure Radiance - Path Radiance

$L = Ltot – Lp$ ……... 2

The path radiance (Lp) can be calculated from satellite bands by assuming that the darkest pixel represents the lowest recorded value and then subtracting that value from all pixel values in the image, this method is called Dark Object Subtraction (DOS) (18).

Since our research requires comparison of satellite images for different time periods, it has become necessary to correct the Sun's distance to Earth as well as to correct the Sun's altitude. To estimate correct reflectance of any material on the surface of the earth, we need to the following:

Convert DNs to Outgoing radiance utilizing radiometric calibration

Estimate incident irradiance (E)

Reflectance (P) = L / E ……... 3

To convert any digital values (DN) to outgoing Radiance, we use the following equation

$L = (DN – B) / G$ ……... 4

Where:

L = Spectral radiance

G = Slope of calibration function (Channel Gain) of metadata

DN = Digital Number (value recorded)

B = intercept of calibration function (Channel Offset) of metadata.

For the second step, the estimation of radiation falling on the surface of the globe is three steps: -

1- Sun elevation correction

Equation 5 is used to complete Sun elevation correction

$E = E_{\circ} * \cos \theta$ ……... 5

2- Earth -Sun distance correction

$E = E_{\circ} / d^2$ ……... 6

Where:

E = Normalized solar irradiance

$E_{\circ}$ = Solar irradiance at mean earth–sun distance

θ = Sun's angle from the zenith

d = Earth–sun distance in astronomical units

3- Combined irradiance correction

$E = E_{\circ} * \cos \theta / d^2$ ……... 7

Finally, by compensation for equations 5 & 8 in equation 4, It can have the reflectance corrected for any object on Earth's surface.

Regarding the implementation of atmospheric correction, Dark Object Subtract (DOS) technique has been chosen to implement these corrections by using ENVI 5.3v. software. So to convert digital number values DNs ranging from 0-256 to reflectance values ranging from 0-1 (17).

The following equation can be used:

$Ls = Lt + Lh$ ……... 8

Where:

Ls = energy reflected

Lt = energy emitted from the ground

Lh= energy from scattering

The purpose of the geometric correction is to correct the position of each pixels and thus to put the ground target in its correct geometric position in the image(25). Remote sensing techniques are often based on ground control points (GCPs) in geometric correction. GCPs are fixed points on Earth's surface, provided they are visible in the image, or can represent features in the image, such as intersections of roads, building corners, airport runways and other stable phenomena. Geometric correction can be done in several methods such as (From a corrected image, from a corrected and drawn map, in addition to by global positioning system (GPS) instrument). Because the satellite images selected in obtaining the objectives of this research have spatial accuracy 30 m, which does not require the use of differential GPS devices. On the other hand, the study area is a large area and mostly unsafe areas, GPS navigator (GARMIN etrex) has been used to perform the geometric correction. After obtaining a high-resolution satellite image from the General Survey Authority of the Quickbird satellite with spatial resolution 0.6 m was corrected geometrically using GPS navigator, after six natural phenomena were identified on this image to represent GCPs and then go to the study area and get its coordinates by GPS as shown in the table 2.

Table 2. Coordinates of GPS navigator

No.	East GPS m	North GPS m
1	**397629**	**3619217**
2	**394185**	**3604198**
3	**387553**	**3630593**
4	**383078**	**3594452**
5	**380630**	**3644071**
6	**361468**	**3603471**

The RMSE is the standard for accuracy of geometric corrections and co-registrations between images in the next steps. it confirmed by (4) that RMSE is usually equal to half pixel size in the modified satellite model. Figure 7 below shows the value of the RMAE which is equal to 0.47 m from the geometric correction of the satellite image 2018 in the Arc GIS 10.2v software. In order to correct all satellite images which used in this research, the image of Landsat OLI 2018 was corrected by the corrected Quickbird image as applied (image to corrected image technique). Eight common points were identified between the two images for the implementation of this process that conducted by utilizing Arc GIS 10.2v software. The results showed that RMSE is equal to 0.40 m as shown in Figures 6, 7, 8 & 9, which enhances confidence of the previous geometric correction by GPS.

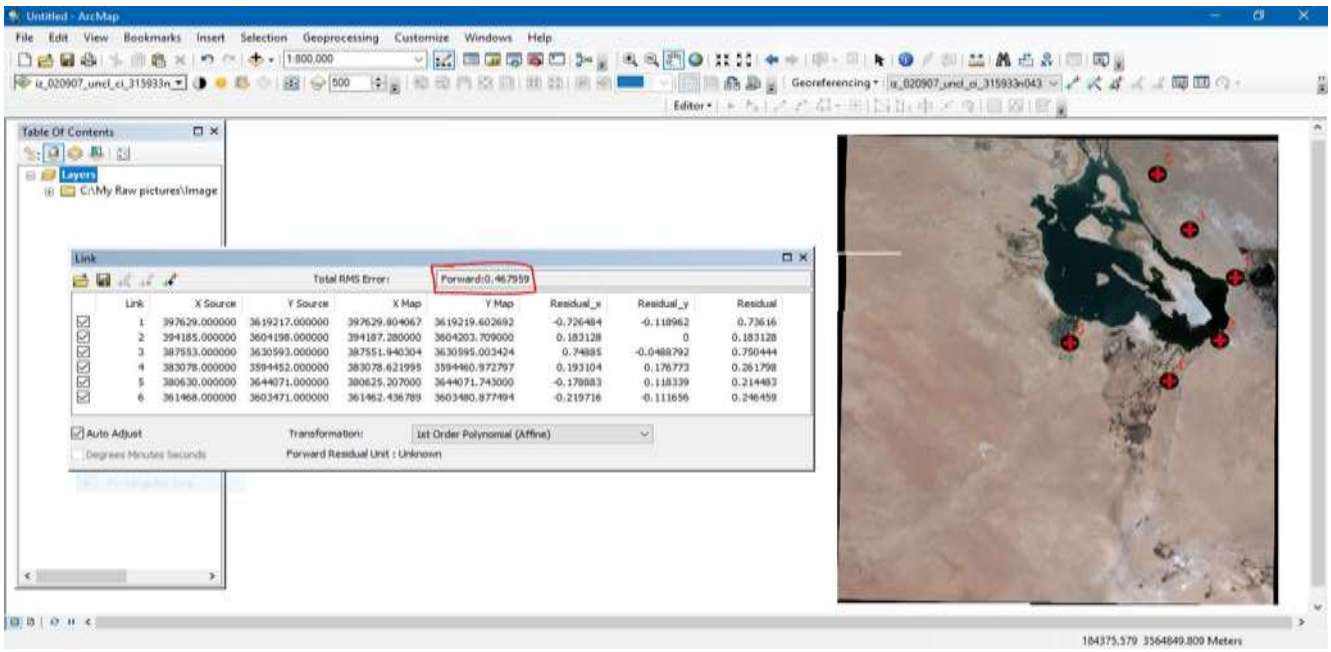

Figure 6. Showing the geometric correction by using Arc GIS 10.2v software

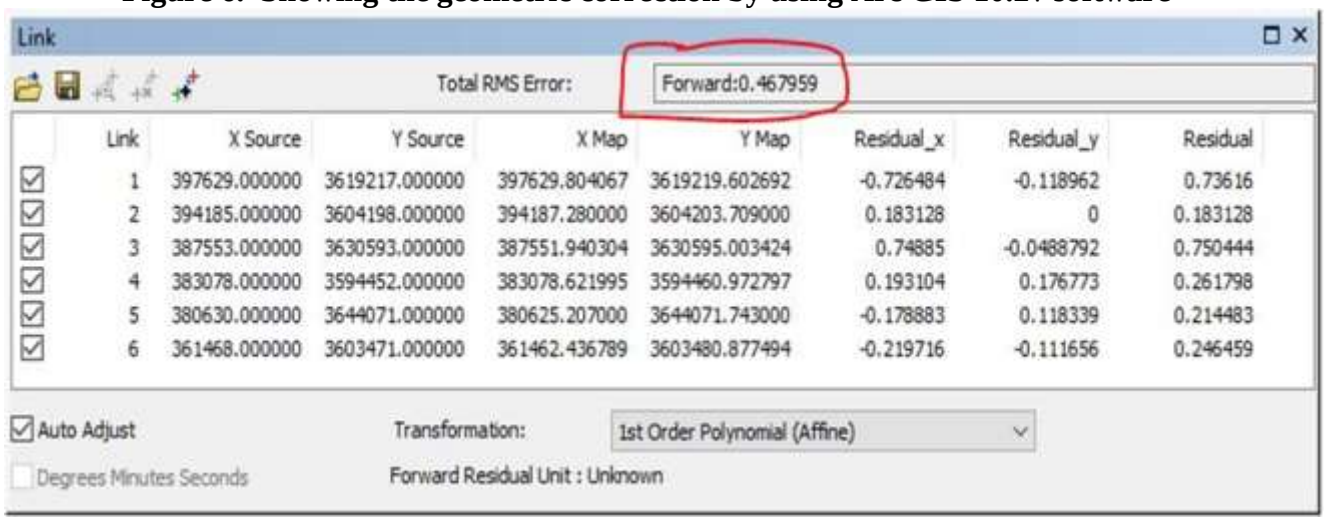

Link	X Source	Y Source	X Map	Y Map	Residual_x	Residual_y	Residual
1	397629.000000	3619217.000000	397629.804067	3619219.602692	-0.726484	-0.118962	0.73616
2	394185.000000	3604198.000000	394187.280000	3604203.709000	0.183128	0	0.183128
3	387553.000000	3630593.000000	387551.940304	3630595.003424	0.74885	-0.0488792	0.750444
4	383078.000000	3594452.000000	383078.621995	3594460.972797	0.193104	0.176773	0.261798
5	380630.000000	3644071.000000	380625.207000	3644071.743000	-0.178883	0.118339	0.214483
6	361468.000000	3603471.000000	361462.436789	3603480.877494	-0.219716	-0.111656	0.246459

Figure 7. RMSE of geometric correction processes

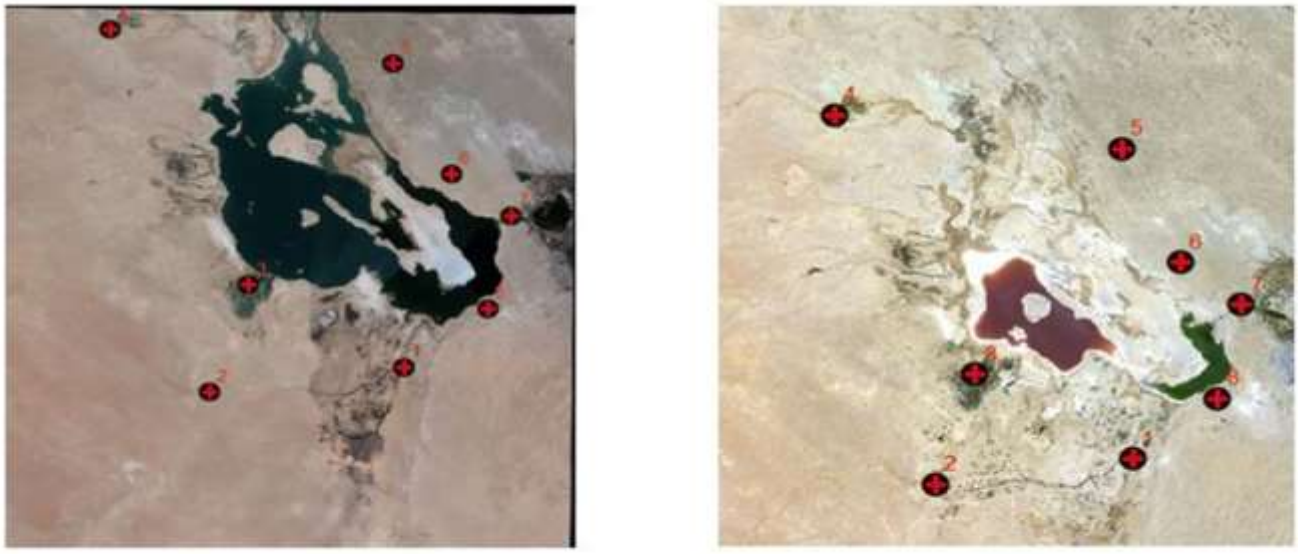

Corrected Quickbird image

Uncorrected Landsat image

Figure 8. Geometric correction process between satellite image 2018 of Landsat 8 OLI and corrected satellite image 2007 of Quickbird for the study area

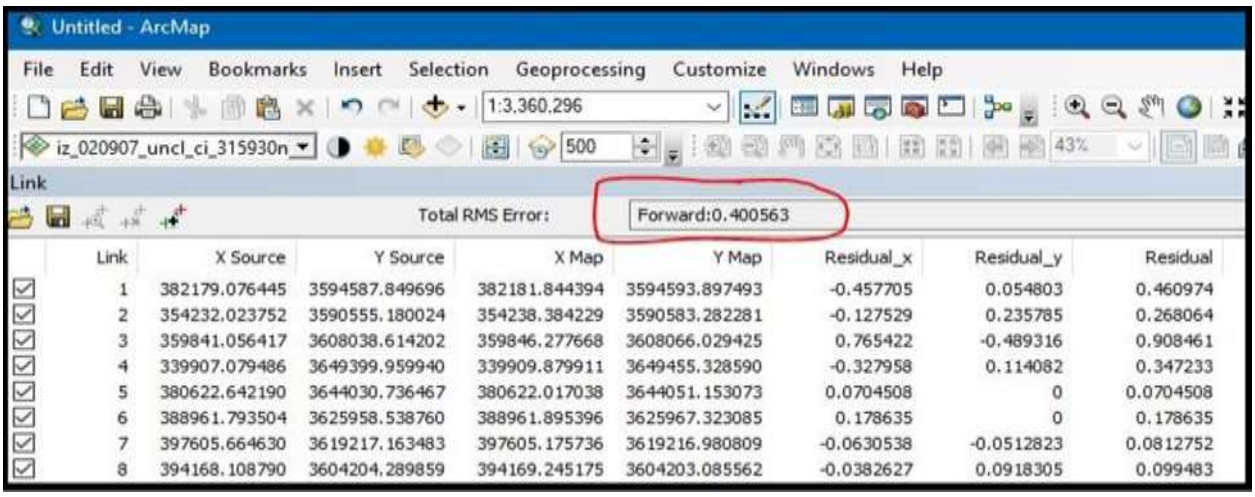

Link	X Source	Y Source	X Map	Y Map	Residual_x	Residual_y	Residual
1	382179.076445	3594587.849696	382181.844394	3594593.897493	-0.457705	0.054803	0.460974
2	354232.023752	3590555.180024	354238.384229	3590583.282281	-0.127529	0.235785	0.268064
3	359841.056417	3608038.614202	359846.277668	3608066.029425	0.765422	-0.489316	0.908461
4	339907.079486	3649399.959940	339909.879911	3649455.328590	-0.327958	0.114082	0.347233
5	380622.642190	3644030.736467	380622.017038	3644051.153073	0.0704508	0	0.0704508
6	388961.793504	3625958.538760	388961.895396	3625967.323085	0.178635	0	0.178635
7	397605.664630	3619217.163483	397605.175736	3619216.980809	-0.0630538	-0.0512823	0.0812752
8	394168.108790	3604204.289859	394169.245175	3604203.085562	-0.0382627	0.0918305	0.099483

Figure 9. RMSE of geometric correction process between two satellite images

After the geometric correction, Registration or Co-registration is the process of alignment of any image to another image of the same region (8). As reported (5) by utilizing this approach leads to gaining of the second image a same geometric error from the first basic image. However, this approach is more appropriate when using multiple-date images to monitor changes on Earth. Accordingly, the registration process for both images (1998 and 2008) to base image 2018 was conducted individually using the ENVI 5.3v software.

Image processing

The second stage of the data processing include Image layers stacking and Sub setting. Layer stacking, that means collecting all bands in a single file for easy opening the image in the program and accelerate the processing (9). The sub setting is defined as the process of take out part of a large file to form one or more small files to simplify and accelerate the analysis in order to obtain the results required as soon as possible. (10). After determining the area of study covering lake Al-Razazzah and its surrounding areas, the steps of images Sub-setting and Resizing were applied by ENVI 5.3v software by select spatial subset by map coordinates shown in the Table 3.

Table 3. Coordinates of sub setting the study area from satellite images

Corner	Longitude	Latitude
Upper left coordinate	**43˚ 19′ 33.50″ E**	**33˚ 08′ 40.68″ N**
Lower right coordinate	**43˚ 55′ 31.02″ E**	**32˚ 23′ 17.42″ N**

SUPERVISED CLASSIFICATION: After completing the radiometric and geometric corrections of the satellite images, the analyst or interpreter can identify homogeneous sets of pixels of similar digital values and divide it into separate sets such as vegetation, water, barren land, etc. (15). One of the supervised classification methods, was chosen as the Support Vector Machine (SVM) to obtain the most accurate results .SVM is one of the most important algorithms used in supervised classification, where nonlinear improvement plays an "effective" role in its methodology (20). It was invented by Vladimir Fabnik and the current version has been updated by Corina Curtis and Vladimir Fabnik (26). The general idea is based on the creation of a hyperplane between datasets to collect data similar to a category indicated by the user. The challenge is to train the machine to understand the structure of the data and plan using the appropriate label for the category for best results (26). Figure 10 identifies the ideal location of the hyperplane which based on the margin value (W)

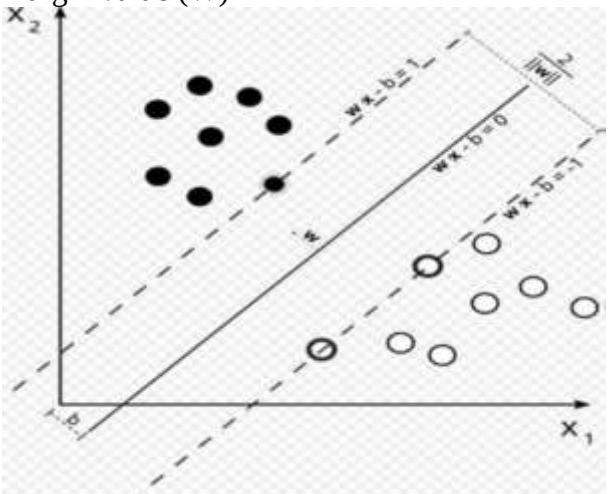

Figure 10. Example of SVM classifier (26).

The mathematical model of SVM as following: (5).

To calculate a training set (T) as defined as follows: $T = \{(pi, qi) \mid pi \in R^n, qi \in \{-1, 1\}, i = 1, \ldots, m\}$ …… 9

Where:

pi = vector of input values

qi = vector of output values

To produce hyperplane H, that separates positive and negative values as:

$W = \sum_{i=0}^{m} mi \cdot qi \cdot pi$ …… 10

Where:

mi = a multiplier

W = normal hyperplane.

Can compensate for any point on the hyperplane as

$w \cdot x + b = 0$ …… 11

Where

b = bias function

As a final result, if any points have n i > 0, are called support vectors.

All stages of the classification were done employing by ENVI 5.3v, after we determine the types of classes within the study area according to "international standards used in land use - land cover (LU/LC) classification. Five major classes were selected Deep water, Shallow water, Agricultural land, Saline Soil and Barren land. In short, shallow water can be described as less than 2 meters deep, while the water more than 2 meters deep is considered a deep water. Then gathered training sites for each selected class by drawing polygons around areas of interest by 30,000 pixels for samples used in the classification process and 10,000 pixels for samples which utilizing, subsequent, in accuracy assessment, according to the limits used to determine the size of the selected samples, it is 70% for the classification process and 30% for the evaluation of accuracy (7). The program performs the direct classification of the corrected satellite image by applying the SVM algorithm using "training sites which entered into the program by the user, where the algorithm matches the spectral signature of each pixel in the image with the sample values of the training to form separate groups that are very similar in order to obtain a classified image (5).

RESULTS AND DISCUSSION

After completing the classification process, the thematic maps for the elected three years were extracted as shown in Figures 11, 12 & 13. From thematic maps, it notes that the images are classified into five main categories and according to global standards, as previously mentioned, and each color was chosen to be close to the natural color of the class. It can also be noted very clearly the extent of the degradation of al Razzazah lake and its negative effects on the surrounding areas.

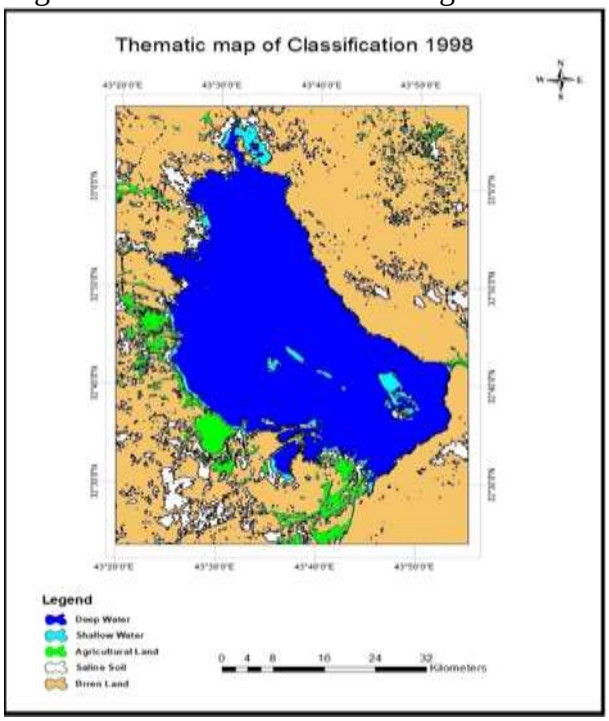

Figure 11. Thematic Map of study area for 1998

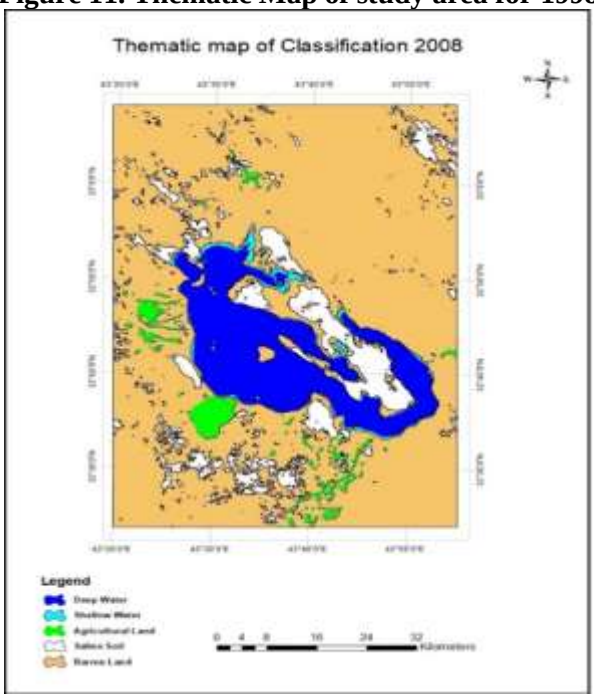

Figure 12. Thematic Map of study area for 2008

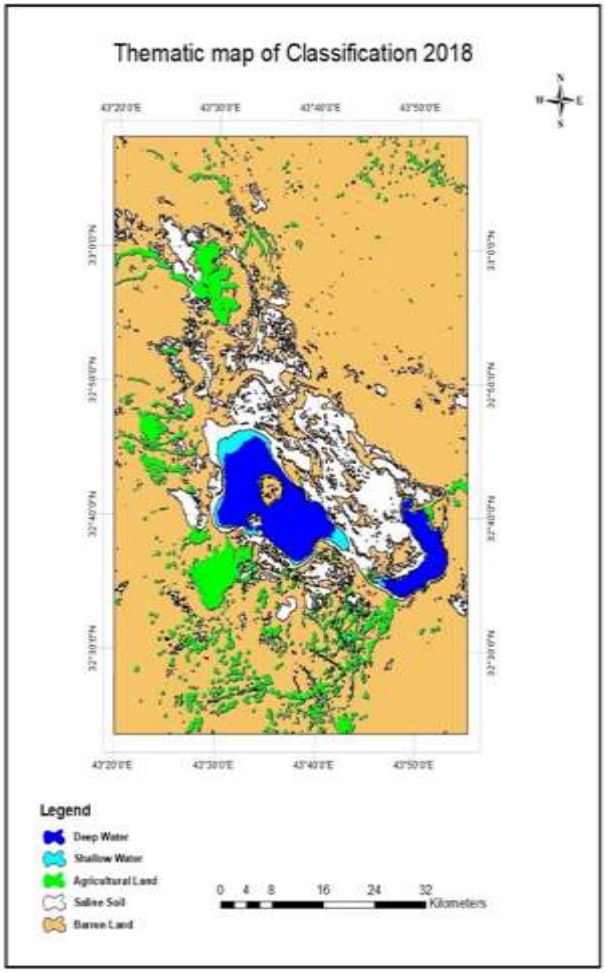

Figure 13. Thematic Map of study area for 2018

Accuracy Assessment of Classification Results

The accuracy assessment is the last step in analyzing the satellite images through which the accuracy of the results obtained can be verified (7). (5, 12) Confirmed that the value of the Kappa coefficient is between 0 - 1, if it is equal to 0 This indicates that there is a strong disagreement between the outputs of the classification and the reference data. In contrast, there is a strong agreement if the value is equal to 1, while if the value ranged from 0.4 - 0.8 the accuracy is medium, and the low value refers to the randomized classification. After the classification process has been completed using the ENVI 5.3v software, the results of accuracy of those classifier images has been assessed and validated and showed it are accepted because of Kappa coefficient is more than 0.80. Confusion matrix for five different classes for the study area is shown in Tables 4, 5, & 6 below:

Table 4. Summary of Land cover of classification accuracies for satellite image 1998

Land Cover Class	TM (9/ 8 / 1998) Producer's	User's
Deep Water	90.14%	95.13%
Shallow Water	90.39%	83.91%
Agricultural Land	91.77%	94.42%
Saline Soil	85.16%	92.32%
Barren Land	93.04%	86.13%
Overall Accuracy	90.11 %	
Kappa Coefficient	0.8764	

Table 5. Summary of Land cover of classification accuracies for satellite image 2008

Land Cover Class	OLI (16 / 8 / 2018) Producer's	User's
Deep Water	87.04%	93.72%
Shallow Water	88.34%	83.72%
Agricultural Land	93.64%	92.40%
Saline Soil	92.34%	90.17%
Barren Land	91.49%	93.50%
Overall Accuracy	90.57 %	
Kappa Coefficient	0.8821	

Table 6. Summary of Land cover of classification accuracies for satellite image 2018

Land Cover Class	TM (4 / 8 / 2008) Producer's	User's
Deep Water	96.26%	94.45%
Shallow Water	84.75%	90.87%
Agricultural Land	90.16%	90.30%
Saline Soil	91.53%	94.03%
Barren Land	95.46%	86.31%
Overall Accuracy	91.60%	
Kappa Coefficient	0.8950	

Change detection analysis and results

One of the most important advantages of remote sensing is its ability to capture, record and store a large amount of information about phenomena on Earth's surface at different conditions and for different periods to benefit

from them in determining and knowing the changes that have taken place, this is called "Change Detection process" , this applies several digital algorithms that calculate the detection of numerical differences in the corresponding pixel values with different dates (12). The same source added that the reliability of the change detection process is affected by several factors, including the different environmental factors that change between the acquisition dates, weather requirements, wind, and soil moisture. The Post Classification Change Detection technique was used to obtain desired results due to the smoothness and accuracy of this method, it naturally requires pre-classified satellite images, where its algorithm compares the corresponding (thematic) pixel labels to detect and identify changes between existing classes. One of the most important features of this method is that it reduces search area and the effects of seasonal variations and atmospheric differences between scenes, in contrast to its most prominent disadvantages, is that classification errors that may exist during classification lead to the discovery of the wrong change (Jensen, 2015).. From Table 7 and Figure 14 changes can be observed in the study area for the period from 1998 to 2008. It can conclude the area of deep water of al Razzazah Lake in 2008 decreased by 786.85520 km², or 57.89% compared to 1998, as well as the shallow water area reduced by 38.69% or 56.386197 km², which in turn clearly affected on the neighboring areas, which led to a minimize in the area of vegetation in all its varieties by 81.56934 km², or 44.55% than in 1998. Accompanied by a clear increase in saline soil, especially "in the land that was covered with water where it increased by 86.544896 km², or 23.29%, In addition to the rise of arid land by 32.09%, an increase of 836.57455 km².

Table 7. Results of Change Detection (1998 - 2008)

Classes	(1998) Area km²	(2008) Area km²	Different km²	Ratio %
Deep Water	1359.15	572.29	-786.85	-57.89
Shallow Water	145.71	89.33	-56. 386	-38.69
Saline Soil	371.47	458.01	+86.544	23.29
Agricultural Land	183.09	101.52	-81.569	-44.55
Barren Land	2606.53	3443.10	+836.57	+32.09
Total Area km²	4665.96	4664.27		

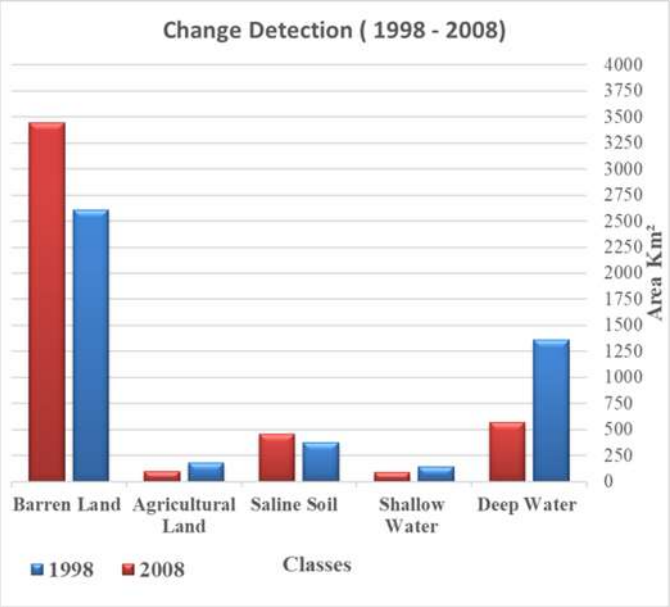

Figure 14. Chart of Change Detection (1998 – 2008)

As for the results of the second stage of the change detection for the period 2008-2018, Table 8 and Figure 13 show that the area of deep water also minimized by 384.932621 km² or 67.26% of its area in 2008 accompanied by a reduction in the area of shallow water by 40.400923 km², or 45.23%, which in turn led to a significant increment in saline soil by 154.82203 km², which means by 33.80%. In addition to a slight increase in the barren lands by 2.31% or 79.576781 km² as a result of the growing in agricultural land, which raised significantly despite the continuous decline in the level of the lake water to reach the increase to 189.74%, or 192.625931 km². This can be explained by that a some of agricultural land owners have followed modern irrigation methods such sprinkler irrigation, as well as increase of areas covered by the cane, shumbolan vegetation and algae, which

usually grow in shallow water and in river stream water. From these result in this research, the large reduction in the surface area of the lake can also be seen by the Figure 16 below.

Table 8. Results of Change Detection (2008 - 2018)

Classes	(2008) Area km²	(2018) Area km²	Different km²	Ratio %
Deep Water	572.29	187.36	-384.932	-67.26
Shallow Water	89.33	48.93	-40.40	-45.23
Saline Soil	458.02	612.84	+154.82	+33.80
Agricultural Land	101.52	294.14	+192.62	+189.74
Barren Land	3443.11	3522.68	+79.57	+2.31
Total Area km²	4664.27	4665.96		

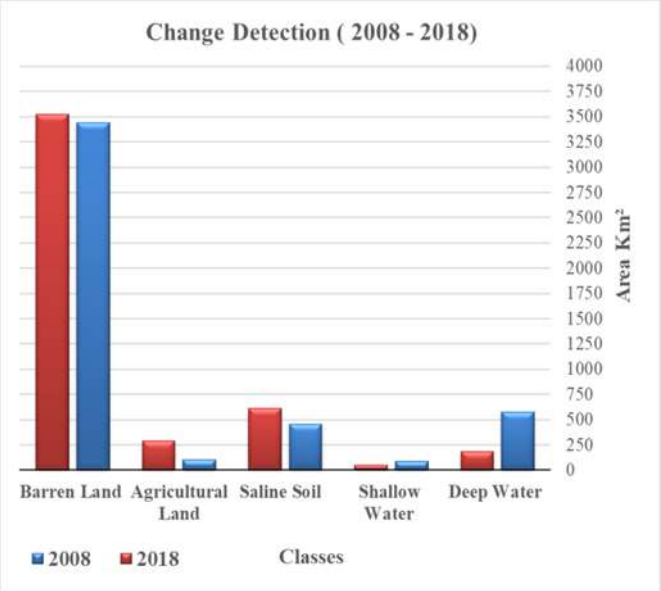

Figure 15. Chart of Change Detection (2008 – 2018)

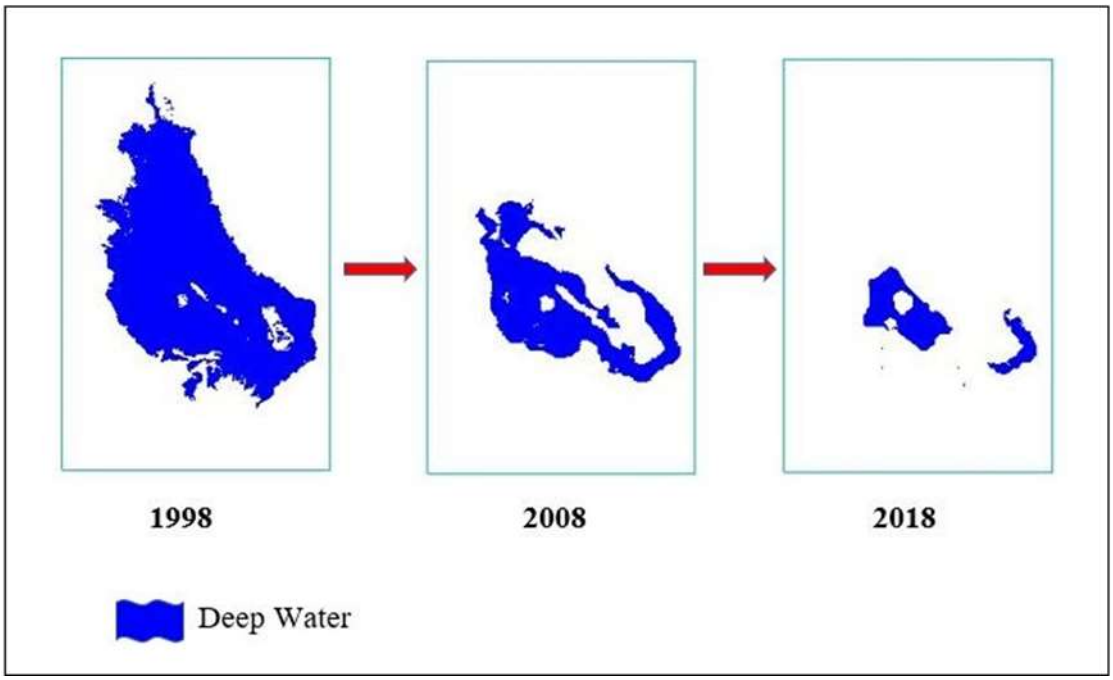

Figure 16 the change in the surface area of the lake for years (1998, 2008 & 2018)

REFERENCES

1. Abdulwahhab, R. A., F. A., Hadi, and M. A. Saleh, 2012. The study of the surface area change of lake Al-Razzaza using geographic Information System (GIS) and using remote sensing technology introduction : objective of The research :, 53(4), 1025–1031

2.Al-dabbas, M. A. 2015. Impact of Climate Changes on the Hydrochemistry of Razaza Lake and Rahaliya – Shithatha Springs – Central Iraq, 5(6).

3. Al-Dabbas, M., Q., Al-Kubaisi, T., Hussein, and S. Al-Qaraghuli, 2018. Hydrochemical properties of ground water of Rahaliya-Ekhedhur region, west Razzaza lake, Iraq. MATEC Web of Conferences, 162, 8–13. https://doi.org/10.1051/matecconf/201816205002

4. Awange, J. L., and J. B. Kyalo Kiema, (2013). Fundamentals of remote sensing. Environmental Science and Engineering (Subseries: Environmental Science), (9783642340840), 111–118. https://doi.org/10.1007/978-3-642-34085-7_7

5. Borra, S., N., Dey, and R. Thanki, 2019. Satellite Image Analysis: Clustering and Classification

6. Bunn, S. E., and A. H. Arthington, 2002. Basic principles and ecological consequences of altered flow regimes for aquatic biodiversity. Environmental Management, 30(4), 492–507. https://doi.org/10.1007/s00267-002-2737-0

7. Canty, M. J. 2009. IMAGE ANALYSIS , in REMOTE SENSING. CRC Press Taylor & Francis Group

8. Chuvieco, E. 2018. Fundamentals of Satellite Remote Sensing. Fundamentals of Satellite Remote Sensing. https://doi.org/10.1201/b18954

9. Dibs, H., M. O., Idrees, and G. B. A. Alsalhin, 2018. Estimating and mapping the rubber trees growth distribution using multi sensor imagery with remote sensing and GIS analysis. Journal of University of Babylon, Pure and Applied Sciences, 26(6), 109–123

10. ERDAS Inc. 1999 'ERDAS Field Guide. Fifth Edition, Revised and Expanded'

11. Ghazal, N. K., A. H.,Shaban, F. K., Mashi, and A. M. Raihan, 2012. Change Detection Study Of Al Razaza Lake Region Utilizing Remote Sensing and GIS Technique, 53(4), 950–957

12. Heydari, S. S., and G. Mountrakis, 2015. remote sensing and image interpretion, Seventh Edition

13. Husain, Y. 2016. Monitoring and Calculating the Surface Area of Lakes in Northern Iraq, 54–62

14. Jaber, H. S., S., Mansor, B., Pradhan, and N. Ahmad, 2017. Rainfall--runoff modelling and water balance analysis for Al-Hindiyah barrage, Iraq using remote sensing and GIS. Geocarto International, 32(12), 1407–1420

15. Jensen, J. R. 2015. introductory digital image processing A remote sensing perspective

16. Llovet, J. M., Ricci, S., Mazzaferro, V., Hilgard, P., Gane, E., Blanc, J.-F., … others. 2008. Sorafenib in advanced hepatocellular carcinoma. New England Journal of Medicine, 359(4), 378–390

17. Lopez, R. D., J. G., Lyon, L. K. Lyon, , and D. K. Lopez, 2013. Wetland Landscape Characterization

18. Mezaainis, V., Jaruzelskl, J., & Wajiullah, M. (n.d.). Advanced Remote Sensing and GIS Advanced Remote Sensing and GIS

19. Othman, A. A., Y. I., Al-Saady, A. K., Al-Khafaji, and R. Gloaguen, 2014. Environmental change detection in the central part of Iraq using remote sensing data and GIS. Arabian Journal of Geosciences, 7(3),1017–1028. https://doi.org/10.1007/s12517-013-0870-0

20. Piccialli, V., and M. Sciandrone, 2018. Nonlinear optimization and support vector machines. 4or, 16(2), 111–149. https://doi.org/10.1007/s10288-018-0378-2

21. Sarp, C. and M Ozcelik, 2016. Water body extraction and change detection using time series : A case study of Lake Burder , Turkey , Integrative Medicine Research. Taibash University, 11(3), pp.381–391.doi:10.1016/j.jtusci.2016.04.005

22. Schowengerdt, R. A. 2007. Remote Sensing: Models and Methods for Image Processing Third Edition

23. Secretariat, R. C. 2013. The Ramsar Convention Manual , 6th edition

24. Tian, B., Y., Zhou, R. M., Thom, H. L., Diefenderfer, and Q. Yuan, 2015. Detecting wetland changes in Shanghai , China using FORMOSAT and Landsat TM imagery. JOURNAL OF HYDROLOGY, 529, 1–10. https://doi.org/10.1016/j.jhydrol.2015.07.007

25. U.S. Geological Survey (USGS). (2013). Landsat 8 Fact Sheet. Fact Sheet 2013-3060, 3–6. Retrieved from http://pubs.usgs.gov/fs/2013/3060/pdf/fs2013-3060.pdf

26. Xie, K. 2011. Support vector machine, concept and matlab build

27. Zaeen, A. A. 2012. Using remote sensing techniques to monitoring and evaluate the water cover in AL _ Razzaza lake : Iraq at deferent periods., 10(17), 45–52.